THE JOURNAL OF PHYSICAL CHEMISTRY Letters

Letter

pubs.acs.org/JPCL

Detection of Negative Charge Carriers in Superfluid Helium Droplets: The Metastable Anions He^{*-} and He_2^{*-}

Andreas Mauracher,[†] Matthias Daxner,[†] Johannes Postler,[†] Stefan E. Huber,[†] Stephan Denifl,[†] Paul Scheier,[†,*] and J. Peter Toennies[‡,*]

[†]Institut für Ionenphysik und Angewandte Physik, Universität Innsbruck, Technikerstr. 25/3, A-6020 Innsbruck, Austria

[‡]Max Planck Institut für Dynamik und Selbstorganisation, Am Fassberg 17, D-37077 Göttingen, Germany

ABSTRACT: Helium droplets provide the possibility to study phenomena at the very low temperatures at which quantum mechanical effects are more pronounced and fewer quantum states have significant occupation probabilities. Understanding the migration of either positive or negative charges in liquid helium is essential to comprehend charge-induced processes in molecular systems embedded in helium droplets. Here, we report the resonant formation of excited metastable atomic and molecular helium anions in superfluid helium droplets upon electron impact. Although the molecular anion is heliophobic and migrates toward the surface of the helium droplet, the excited metastable atomic helium anion is bound within the helium droplet and exhibits high mobility. The atomic anion is shown to be responsible for the formation of molecular dopant anions upon charge transfer and thus, we clarify the nature of the previously unidentified fast exotic negative charge carrier found in bulk liquid helium.

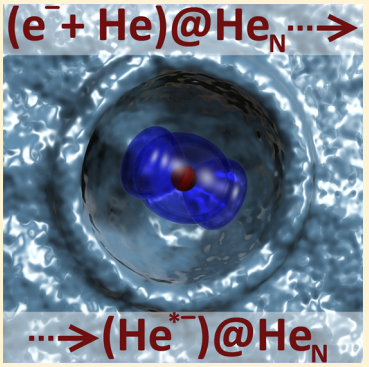

SECTION: Liquids; Chemical and Dynamical Processes in Solution

A wealth of detailed information on charged and neutral, atomic and molecular systems has been provided by low temperature experiments utilizing the helium droplet technique in recent decades.[1] To fully understand the ion−molecule reactions in helium droplets, a detailed knowledge of the charge-transfer mechanism is of fundamental importance. For positive charges, this proceeds via a resonant charge-hopping process[2] that is terminated either by irreversibly forming a molecular helium cation[3] or by ionization of the dopant.[4] The situation is different for negative charges. Electrons solvated in liquid helium and in helium droplets form bubbles[5] with a radius in a range of 11−15 Å.[6] In the low energy range (<20 eV), the formation of anions of molecules embedded in helium droplets is expected to occur via direct interaction with electrons and via intermediate metastable electronic excitation of a helium atom.[7] At higher electron energies (>20 eV), direct electron interaction is the dominant mechanism.[8]

The observation of unusually fast negative ions in bulk helium was first reported in 1969. However, in these ion mobility experiments, the anions could not be assigned.[9] Two years later, their existence was confirmed and these exotic fast negative carriers (EFNCs) were assigned to the anion He(1s2s2p ^{4}P) (denoted simply as He^{*-} in the following).[10] Since then, alternative assignments have been suggested for the EFNC, specifically to bubbles containing two electrons[11] and most recently to He_2 ($1\sigma_g^2\ 1\sigma_u\ 2\sigma_g\ 1\pi_u\ ^4\Pi_g$) anions (denoted simply as He_2^{*-} in the following).[12] He^{*-} and He_2^{*-} have been intensively studied in the gas phase both by experiment[13,14] and by theory.[15,16]

For the present work, it is essential to recall the following facts. The atomic anion consists of an excited metastable state He(1s2s ^{3}S) (denoted simply as He* in the following), which due to its positive electron affinity of 77 meV can attach an electron.[15] He^{*-} shows the characteristics of a He^+ core surrounded by two loosely bound electrons.[17] The molecular helium anion has a similar structure. The electronically excited metastable state He_2 ($1\sigma_g^2\ 1\sigma_u\ 2\sigma_g\ ^3\Sigma_u^+$) (simply denoted as He_2* in the following) has a positive electron affinity of 0.233 eV.[18] The lifetimes of He^{*-} and He_2^{*-} in the gas phase have been measured as 359.0 ± 0.7 μs (for the total angular momentum quantum number J = 5/2)[19] and 135 ± 15 μs,[14] respectively.

In this paper, we use an apparatus[8] in which a beam of pure neutral superfluid helium droplets is crossed with a beam of magnetically guided electrons of defined energy with an electron energy resolution <1 eV. The electron impact energy was varied in a range from 19 to 59 eV. The anions formed at a certain electron impact energy are then analyzed according to their mass-to-charge ratio utilizing a time-of-flight mass spectrometer. From various mass spectra at different electron impact energies, anion efficiency curves can be derived. In these experiments, new insight into the physics of anion formation in helium droplets is gained by varying the mean size of the helium droplets by changing the helium droplet source conditions (stagnation pressure and nozzle temperature)[8] as well as the impact energy of the electrons. In addition, we dope the pure neutral helium droplets with sulfur hexafluoride, SF_6,

Received: May 9, 2014
Accepted: June 20, 2014
Published: June 20, 2014

   dx.doi.org/10.1021/jz500917z | J. Phys. Chem. Lett. 2014, 5, 2444−2449

in order to explore the mobility of the helium anions and to reveal their role in charge transfer processes.

We find that the negative mass spectra of pure helium droplets ($N \approx 2.4 \times 10^6$, N denotes the number of helium atoms in the helium droplet) measured with an electron impact energy of 22 eV are dominated by an intense He^{*-} anion peak and a peak from He_2^{*-} which is 2 orders of magnitude smaller. The ion efficiency curves for both anions as a function of the electron impact energy are shown in Figure 1a. For a better comparison of the yield of He^{*-} with He_2^{*-} we multiplied the latter signal by a factor of 100. To analyze the resonant structure of He^{*-} we fitted a triple-Gaussian function to reproduce the ion yield around 22 eV electron impact energy, which yields positions of maxima located at 22.0 ± 0.2 eV, 23.0 ± 0.2 eV, and 25.1 ± 0.5 eV, respectively.

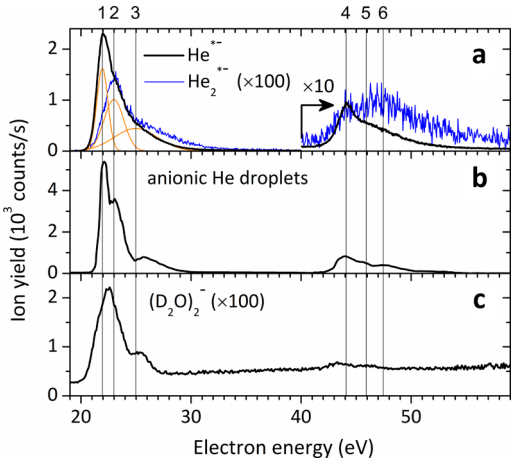

Figure 1. (a) He^{*-} (black line) and He_2^{*-} (blue line) yields measured with I_{el} = 60 μA for droplets with $N \approx 10^6$ (T_0 = 8.5 K, P_0 = 23 bar). (b) Total negative ion yield measured with an electron current of I_{el} = 20 μA for droplets with $N \approx 5 \times 10^5$.[20] (c) Yield of heavy water dimer anions in droplets with $N \approx 10^4$.[21] The ochre Gaussian peaks, which were fitted to the black He^{*-} peak, agree well with the structures in the other curves.

The three positions of the maxima are indicated with vertical, numbered lines in Figure 1a. Three similar resonances are found about 22 eV higher in energy and are marked with vertical, numbered lines as well. These values are in good agreement with earlier reported maxima of resonant formation of anionic helium droplets,[20] shown in Figure 1b. Figure 1c represents the ion yield of dimer anions, $(D_2O)_2^-$,[21] from helium droplets doped with heavy water. The behavior of these anions is characteristic of many negatively charged molecules and clusters extracted from doped helium droplets.[22−24] The results of these two studies are presented to emphasize the role of helium anions for charge transfer reactions. The positions of all resonance maxima measured here are compared with earlier work for creation of negative droplets and water dimer anions $(D_2O)_2^-$ in Table 1 and agree remarkably well.

The present experiments indicate that the formation of helium anions proceeds via a two-step reaction. First, the electron penetrates the surface of the helium droplet and excites a ground state helium to its first excited state to form a He* and a low-energy electron localized in a bubble. Because of the attractive polarization forces He* (which is about 200 times more polarizable than ground state helium)[25] and the electron combine and form He^{*-}, as illustrated in Figure 2. As recently discussed,[26] both He* and He^{*-} form large voids inside the helium droplet. The combination of He* with the electron is energetically favored since the total energy of a single bubble is less than that of two separate bubbles.[27] A single-step process seems to be highly unlikely, that is, the instantaneously attachment of the free electron with the excitation of the ground state helium to He*, because the formation of a helium anion in the gas phase has not been reported yet.

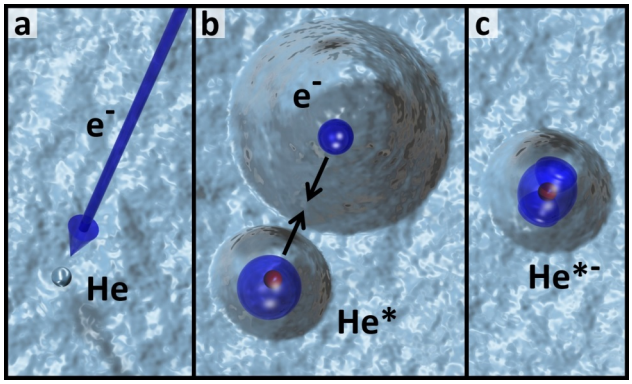

Figure 2. Cartoon showing steps in the formation of helium anions in a helium droplet. (a) Electron with an initial kinetic energy of 22 eV penetrates the helium droplet and excites a ground state helium to He*. Because of penetration of the helium droplet and the excitation of a ground state helium, the electron has virtually no kinetic energy after localization in an electron bubble. (b) Polarizable He* and the electron bubble move toward each other due to charge-dipole-induced forces. (c) He* and the electron bubble combine and form a He^{*-}. The blue background is to indicate the helium environment and to illustrate the formation of voids.

Table 1. Positions of the Resonance Maxima (in eV) and Relative Intensities in Brackets[a]

peak number (Figure 1)	He^{*-} [b]	He_2^{*-} [b]	negative droplets[c]	$(D_2O)_2^-$ [d]
			2.1 ± 0.1 [0.52]	1.55 ± 0.2 [1.00]
1	22.0 ± 0.2 [1.00]		22.3 ± 0.1 [1.00]	22.4 ± 0.5 [0.63]
2	23.0 ± 0.2 [0.57]	22.9 ± 0.2 [1.00]	23.3 ± 0.1 [0.70]	
3	25.1 ± 0.5 [0.23]	24.8 ± 0.5 [0.34]	25.6 ± 0.4 [0.15]	25.0 ± 0.5 [0.16]
4	44.0 ± 0.2 [0.032]	43.8 ± 0.2 [0.028]	44.0 ± 0.2 [0.009]	43.4 ± 0.2 [0.046]
5	45.5 ± 0.2 [0.022]		45.5 ± 0.2 [0.092]	
6	47.2 ± 0.2 [0.019]	46.7 ± 0.2 [0.049]	51.8 ± 0.5 [0.016]	46 ± 0.2 [0.027]
		50.0 ± 0.5 [0.030]		49.7 ± 0.5 [0.013]

[a]The intensities are normalized to the largest peak in each of the spectra. [b]This work. [c]Data from ref 20. The position depends somewhat on the droplet size. [d]Data from ref 21.

dx.doi.org/10.1021/jz500917z | J. Phys. Chem. Lett. 2014, 5, 2444−2449

Considering the energy needed for the electron to penetrate the surface of the helium droplet (1.2 eV)[28] and the excitation energy required to form He* (19.8 eV) from ground state helium, the total electron impact energy required to form He^{*-} inside a helium droplet sums up to 21 eV, which corresponds to the onset of the first resonance found in the ion efficiency curve of He^{*-}. The second and third maxima correspond to higher excited states of the helium atom, which we calculated employing the equation-of-motion couple-cluster method with single and double substitutions from the Hartree−Fock determinant (EOM-CCSD)[29] and a for helium anions designed basis set with multiply augmented diffuse functions.[26] At this level of theory, the second and third excited states of helium require energies of 20.9 eV for He(1s2p ^{3}P) and 22.7 eV for He(1s3s ^{3}S), respectively, to be formed from ground state helium. These values are in good agreement with known experimental values of 20.964 eV for He(1s2p ^{3}P) and 22.72 eV for He(1s3s ^{3}S), respectively.[30] Also, higher excited states will contribute to the ion formation of He^{*-}. However, these states are too close in energy to be resolved with the electron energy resolution of our ion source, which is <1 eV. Therefore, we took into account only the first three excited states in the fitting procedure. The higher excited states which are close in energy contribute to the width of the third resonance, which is notably larger than for the first two resonances. For He_2^{*-}, only two resonance maxima can be observed centered at 22.9 ± 0.2 eV and 24.8 ± 0.5 eV.

The formation of He_2^* or He_2^{*-} cannot proceed via dimerization from a He* or He^{*-} and a helium ground state atom due to barriers that cannot be overcome at the low temperatures present in the helium droplets (0.37 K).[26] Again we use EOM-CCSD to explore the potential energy curves for the interaction of a helium ground state atom with the 12 lowest excited states of the atomic helium. In perfect agreement to the experimental results, we find that there exist only two excited states of the atomic helium that lead to a barrier-free dimerization with a ground state helium atom to produce an excited molecular helium. Only these excited states can attach an electron to form a molecular helium anion. The two states are He(1s2p ^{3}P) and He(1s3p ^{3}P) with an excitation energy of 20.9 and 23.0 eV, respectively. Considering the energy of 1.2 eV[28] required for the electron to penetrate the helium droplet surface we arrive at energies for the formation of He_2^{*-} of 22.1 and 24.2 eV, respectively, which are in reasonable agreement with the experimental findings.[31]

We now turn to a key property of the two anionic helium species: their mobility inside helium droplets. Insight can be obtained from the negative charging of the heliophilic dopant SF_6, which is located near the droplet center.[32] In Figure 3a, we show the ion yield of He^{*-}, He_2^{*-}, and SF_5^- as a function of the pressure of SF_6 in the pick-up chamber and therefore as a function of the average number of SF_6 molecules picked up by the helium droplets. The increase in the SF_5^- ion yield corresponds nicely to the exponential drop in the He^{*-} yield, which suggests that He^{*-} is highly mobile. The exponential decrease over more than 2 orders of magnitude corresponds exactly to the probability that the helium droplet does not pick up any SF_6 molecules in the pick-up cell. In contrast, the two higher excited atomic helium anions formed at 23.0 and 25.1 eV, respectively, (states labeled 2 and 3 in Figure 3b) are less affected and the molecular helium anions are almost entirely unaffected (Figure 3a) by the presence of SF_6 inside the helium droplet and are, therefore, far less mobile.

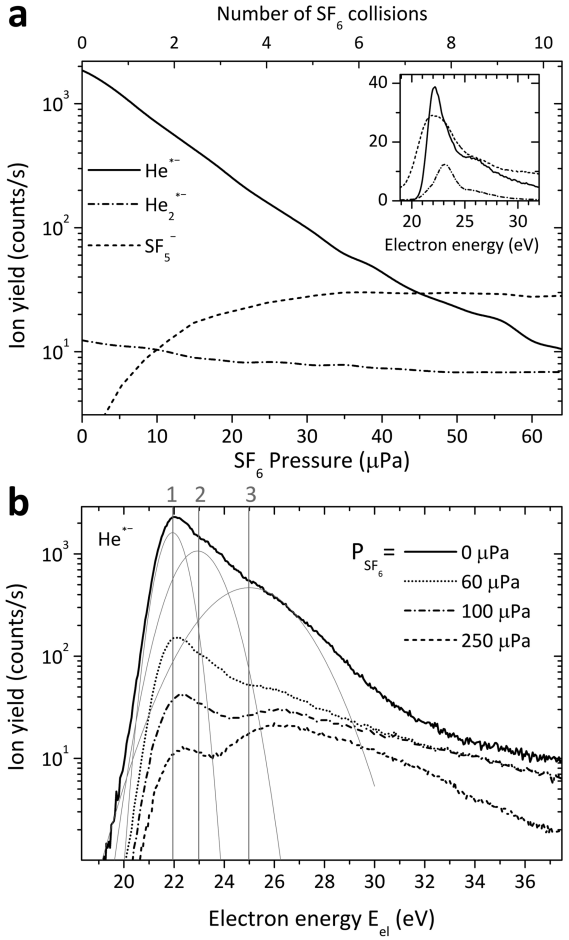

Figure 3. (a) Yield of He^{*-} (solid curve), He_2^{*-} (dash-dotted curve), and SF_5^- (short-dashed curve) in a log scale as a function of increasing pressures of SF_6 gas in the scattering chamber (I_{el} = 50 μA). The ions were formed at an electron impact energy of 22 eV in droplets with $N \approx 10^6$ (T_0 = 8.5 K, P_0 = 23 bar). The SF_6 pressure is converted into the probable number of SF_6 collisions displayed on the top abscissa. The small inset shows the resonant structure of the yield for He^{*-} (solid curve), He_2^{*-} (short-dashed curve), and SF_5^- (dash-dotted curve) measured under the same conditions. (b) Yield of He^{*-} as a function of the electron energy for various SF_6 pressures. The three resonances are marked with gray lines. Those labeled 2 and 3 are less effected by the SF_6 pressure than the resonance 1.

As estimated in ref 20 from the total electron scattering cross section,[33] the anionic helium species will be created near the surface of a droplet with a maximum probability at a depth of about D = 1.5−2.5 nm. This depth is well defined because as electrons penetrate deeper they lose energy and are no longer in resonance. Because D is small compared to the radius of 37.7 nm of an $N = 5 \times 10^6$ helium droplet the anions will need to travel 15−25 times the penetration depth to reach and react with an SF_6 molecule or cluster. Considering the polarizability of SF_6 (6.55 Å^3)[34] in comparison to the polarizability of He* (46.77 Å^3),[25] as well as the distances between the electron bubble and the two mentioned species, it is reasonable that He^{*-} will be formed instead of the electron bubble migrating toward the dopant in the center of the helium droplet. The charge transfer from He^{*-} to the embedded molecules is also reflected in the similar shape of the ion efficiency curves of He^{*-} and the embedded molecular anion (see inset in Figure 3). The ion yield of SF_5^- below 20 eV arises from low-energy

dx.doi.org/10.1021/jz500917z | J. Phys. Chem. Lett. 2014, 5, 2444−2449

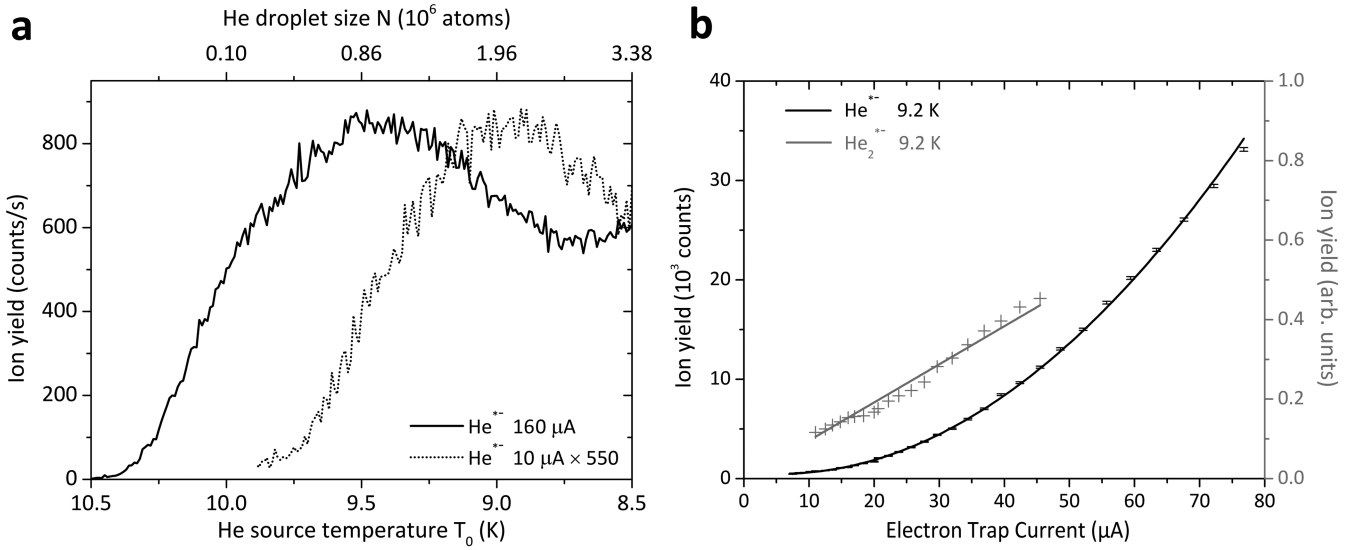

Figure 4. (a) Droplet size dependence of the helium anion yields measured for P_0 = 23 bar and an electron current of I_{el} = 160 μA (solid line) and I_{el} = 10 μA (dotted line), respectively. (b) Electron current dependence of the helium anion yield measured for P_0 = 23 bar and T_0 = 9 K (black solid line) and of the molecular anion yield measured at the same conditions (gray solid line). The best fits can be achieved with quadratic function for the atomic helium anion and a linear function for the molecular helium anion. The electron energies were chosen at the peak of the distributions shown in Figure 1a.

electrons which are formed upon inelastic electron scattering with surface helium atoms and then react with SF_6 molecules near the surface which are present in the case of multiple doping of the helium droplet.

Not only is $He_2{}^{*-}$ less mobile than He^{*-} but also heliophobic. Inspection[26] of the potential energy landscape of the two anionic species experienced by additional helium atoms, computed at the CCSD(T)[35] level of theory, reveals that the energy required to form the repulsive void around the molecular helium anion, in which no other ground state helium atom is found, is larger than the energy gained by surrounding the molecular helium anion with ground state helium atoms. The calculations reveal an opposite trend for the atomic helium anion. In this case, the energy gained by surrounding the anion is 2.75 times larger than the energy required to form the repulsive void. Therefore, the atomic helium anion is not only more mobile than the molecular helium anion, but the molecular helium anion will also be located on the surface of the helium droplet. According to our calculations, the interaction of $He_2{}^{*-}$ with dopants embedded in the center of the helium droplets is strongly suppressed energetically as reflected in the nearly constant $He_2{}^{*-}$ yield even at highest SF_6 pressures in the pick-up chamber. The repulsive region in the potential energy landscape around the anionic helium species is a direct measure for the repulsive void formed inside helium droplets. The volumes of these repulsive voids are 838.46 Å^3 for He^{*-} and 8480.6 Å^3 for $He_2{}^{*-}$, respectively. The volume of the repulsive void for He^{*-} corresponds to an effective radius of 5.85 Å, which is close to the reported radius of the EFNC of 7.3 Å.[36]

The high mobility and energetically favored situation of He^{*-}, once it is surrounded by many helium ground state atoms, seems to be in contrast with the observation of He^{*-} in the mass spectra. Therefore, we ask the question how are (these) anions ejected from the helium droplets? In Figure 4a, we show the dependence of the He^{*-} signal on the nozzle temperature and therefore the average helium droplet size. The electron impact energy was fixed at 22 eV for these measurements but two different electron currents, 160 and 10 μA, were employed. Both curves show a similar size dependence, but the onset for the He^{*-} in these nozzle temperature scans is shifted to smaller cluster sizes for the higher electron current. The shift of the two curves is related to the probability of hitting one helium droplet with more than one electron.

In Figure 4b we show the ion yield of He^{*-} at a fixed electron impact energy as a function of the electron current for various droplet sizes. The quadratic dependence suggests that the He^{*-} is released from large helium droplets via Coulomb repulsion from a second negatively charged species (i.e., electron bubble, He^{*-} or $He_2{}^{*-}$). This expulsion mechanism will also apply for other anions embedded in the helium droplets. In comparison, the yield of $He_2{}^{*-}$ shows a linear dependence on the electron current, indicating that this ion resides on the surface, where it is simply desorbed due to the very weak interaction energies of $He_2{}^{*-}$ with the neutral helium droplet.

The evidence of resonant He^{*-} and $He_2{}^{*-}$ formation in helium droplets upon electron impact and their remarkable mobility in helium droplets are the key findings of this experiment. This study provides the first clear evidence for the helium anion formation in helium droplets. The experiments and the calculations show that He^{*-} is heliophilic, is highly mobile, and has a radius similar to that of the EFNC, thereby identifying it as the EFNC reported in bulk liquid helium. Using the example of SF_6, the experiments show that dopant anions created at electron impact energies of about 22 eV are mediated by highly mobile He^{*-} anions and not by electron bubbles, as previously assumed.[20] The single electron transfer from a He^{*-} to a dopant embedded in helium droplets suggests the possibility that the two loosely bound electrons around the He^+-core might open a new approach to form metastable aggregates of dianions in a well-defined quantum-mechanical regime.

dx.doi.org/10.1021/jz500917z | J. Phys. Chem. Lett. 2014, 5, 2444−2449

EXPERIMENTAL METHODS

In the apparatus,[37] neutral pure He droplets, which were shown to be very cold (0.37 K) and superfluid,[38] are produced in a free jet of precooled ^{4}He gas. After passing through the 20.6 cm long pick-up region, the droplets are bombarded by a magnetically guided electron beam with an electron energy resolution of 1 eV in a Nier-type ionizer. The newly formed negative ions are extracted by an electric field of about 50 V/cm and then accelerated to about 40 eV and focused into a commercial reflection time-of-flight mass spectrometer with a mass resolution $m/\Delta m \geq 2000$. There the ions undergo pulsed acceleration and are detected after a distance of about 1 m, which corresponds to flight times of about 3.3 μs (He^{*-}) and 4.6 μs (He_2^{*-}), which are much less than the lifetimes of these anions.

COMPUTATIONAL METHODS

All calculations employed a specialized multiply augmented basis set based on the d-aug-cc-pVXZ, X = *T*, Q of Woon and Dunning,[39] but using a global scaling with a factor of 1/3 for the exponents of the diffuse functions (beyond the second least diffuse one) instead of angular-momentum-dependent scaling factors. The interaction energy between He_2^{*-} and a helium atom was derived at the CCSD(T) level of theory and corrected for the basis set superposition error.[40] Quantum chemical calculations concerning the energy of excited states were performed using the equation-of-motion coupled-cluster approach with single and double excitations based on a single Hartree−Fock determinant. As a reference state, we used the singlet ground state wave function of the molecular helium. As target states, the lowest lying triplet configurations were investigated. All calculations were carried out with the Gaussian 09 suite of programs.[41]

AUTHOR INFORMATION

Corresponding Authors

*P. Scheier. E-mail: paul.scheier@uibk.ac.at. Phone: +43 512 507 52260. Fax: +43 512 507 2922.
*J. P. Toennies. E-mail: jtoenni@gwdg.de. Phone: +49 551 5176 600. Fax: +49 551 5176 575.

Notes

The authors declare no competing financial interest.

ACKNOWLEDGMENTS

We thank Hartmut Hotop for enlightening discussions, a critical reading, and several excellent suggestions, Peter McClintock and Humphrey Maris for their insightful comments, and Klaus Bartschat for preprints and correspondence. This work was supported by the Austrian Science Fund (FWF) Wien (P23657, P24443, P26635, and I978), the Austrian Ministry of Science (BMWF) as part of the Uni-Infrastrukturprogramm of the Research Platform Scientific Computing at the University of Innsbruck (DK+ project Computational Interdisciplinary Modelling, W1227-N16).

REFERENCES

(1) Yang, S.; Ellis, A. M. Helium Droplets: a Chemistry Perspective. *Chem. Soc. Rev.* **2013**, *42*, 472−484.
(2) Scheidemann, A.; Schilling, B.; Toennies, J. P. Anomalies in the Reactions of He^+ with SF_6 Embedded in Large Helium-4 Clusters. *J. Chem. Phys.* **1993**, *97*, 2128−2138.
(3) Callicoatt, B. E.; Förde, K.; Ruchti, T.; Jung, L.; Kenneth, C. J. Capture and Ionization of Argon within Liquid Helium Droplets. *J. Chem. Phys.* **1998**, *108*, 9371−9382.
(4) Ellis, A. M.; Yang, S. Model for the Charge-Transfer Probability in Helium Nanodroplets Following Electron Impact Ionization. *Phys. Rev. A* **2007**, *76*, 032714−8.
(5) Kupfer, C. G. Theory of Negative Ions in Liquid Helium. *Phys. Rev.* **1961**, *122*, 1007−1011.
(6) Poitrenaud, J.; Williams, F. I. B. Precise Measurement of Effective Mass of Positive and Negative Charge Carriers in Liquid Helium II. *Phys. Rev. Lett.* **1972**, *29*, 1230−1232.
(7) Denifl, S.; Zappa, F.; Mähr, I.; Lecointre, J.; Probst, M.; Märk, T. D.; Scheier, P. Mass Spectrometric Investigation of Anions Formed upon Free Electron Attachment to Nucleobase Molecules and Clusters Embedded in Superfluid Helium Droplets. *Phys. Rev. Lett.* **2006**, *97*, 043201−4.
(8) Schöbel, H.; Bartl, P.; Leidlmair, C.; Daxner, M.; Zöttl, S.; Denifl, S.; Märk, T. D.; Scheier, P.; Spångberg, D.; Mauracher, A.; et al. Sequential Penning Ionization: Harvesting Energy with Ions. *Phys. Rev. Lett.* **2010**, *105*, 243402−4.
(9) Doake, C. S. M.; Gribbon, P. W. F. Fast Ions in Liquid Helium. *Phys. Lett. A* **1969**, *30*, 252−253.
(10) Ihas, G. G.; Sanders, T. M. Exotic Negative Carriers in Liquid Helium. *Phys. Rev. Lett.* **1971**, *27*, 383−386.
(11) Sanders, T. M.; Ihas, G. G. Nature of Exotic Negative Carriers in Superfluid ^{4}He. *Phys. Rev. Lett.* **1987**, *59*, 1722−1725.
(12) Khrapak, A. G.; Schmidt, W. F. Negative Ions in Liquid Helium. *Low Temp. Phys.* **2011**, *37*, 387−391.
(13) Schmidt, H. T.; Reinhed, P.; Orbán, A.; Rosén, S.; Thomas, R. D.; Johansson, H. A. B.; Werner, J.; Misra, D.; Björhage, M.; Brännholm, L.; et al. The Lifetime of the Helium Anion. *J. Phys.: Conf. Ser.* **2012**, *388*, 012006−8.
(14) Andersen, T.; Andersen, L. H.; Bjerre, N.; Hvelplund, P.; Posthumus, J. H. Lifetime Measurements of He_2^- by Means of a Heavy-Ion Storage Ring. *J. Phys. B: At. Mol. Opt. Phys.* **1994**, *27*, 1135−1142.
(15) Brage, T.; Froese-Fischer, C. Autodetachment of Negative Ions. *Phys. Rev. A* **1991**, *44*, 72−79.
(16) Adamowicz, L.; Pluta, T. Metastable He_2^- Ions Formed by Two-Electron Attachment to the Excited He_2^+ $^2\Sigma_g^+$ ($1\sigma_g^2 2\sigma_g^1$) Core. *Phys. Rev. A* **1991**, *44*, 2860−2867.
(17) Mercero, J. M.; Elorza, J. M.; Ugalde, J. M.; Boyd, R. J. Electronic Structures of the Bound Excited Quartet States of the Helium Anion. *Phys. Rev. A* **1999**, *60*, 4375−4378.
(18) Michels, H. H. Electronic Structure of the Helium Molecular Anion He_2^-. *Phys. Rev. Lett.* **1984**, *52*, 1413−1416.
(19) Reinheld, P.; Orbán, A.; Werner, J.; Rosén, S.; Thomas, R. D.; Kashperka, I.; Johansson, H. A. B.; Misra, D.; Brännholm, L.; Björkhage, M.; et al. Precision Lifetime Measurements of He^- in a Cryogenic Electrostatic Ion-Beam Trap. *Phys. Rev. Lett.* **2009**, *103*, 213002−4.
(20) Henne, U.; Toennies, J. P. Electron Capture by Large Helium Droplets. *J. Chem. Phys.* **1998**, *108*, 9327−9338.
(21) Zappa, F.; Denifl, S.; Mähr, I.; Bacher, A.; Echt, O.; Märk, T. D.; Scheier, P. Ultracold Water Cluster Anions. *J. Am. Chem. Soc.* **2008**, *130*, 5573−5578.
(22) Denifl, S.; Zappa, F.; Mähr, I.; Mauracher, A.; Probst, M.; Märk, T. D.; Scheier, P. Inelastic Electron Interaction with Chloroform Clusters Embedded in Helium Droplets. *J. Am. Chem. Soc.* **2008**, *15/130*, 5065−5071.
(23) Echt, O.; Märk, T. D; Scheier, P. *Handbook of Nanophysics: Clusters and Fullerenes*; CRC Press: Boca Raton, FL, 2010.
(24) Denifl, S. Formation of Cations and Anions upon Electron Interaction with (Doped) Helium Droplets. *Eur. Phys. J.: Spec. Top.* **2013**, *222*, 2017−2033.
(25) Chen, M.-K. Dipole Polarizabilities of the 1, 2^1S and 2^3S States of the Helium Sequence. *J. Phys. B: At. Mol. Opt. Phys.* **1995**, *28*, 1349−1355.

(26) Huber, S. E.; Mauracher, A. On the Properties of Charged and Neutral, Atomic and Molecular Helium Species in Helium Nanodroplets: Interpreting Recent Experiments. *Mol. Phys.* **2014**, *112*, 794−804.
(27) Ancilotto, F.; Lerner, P. B.; Cole, M. W. Physics of Solvation. *J. Low Temp. Phys.* **1995**, *101*, 1123−1146.
(28) Martini, K.; Toennies, J. P.; Winkler, C. Electron Scattering from ^{4}He and Ne Clusters: Determination of the Cluster Density from the Electronic Surface Barrier Potential. *Chem. Phys. Lett.* **1991**, *178/4*, 429−434.
(29) Stanton, J. F.; Bartlett, R. J. Equation of Motion Coupled-Cluster Method: A Systematic Biorthogonal Approach to Molecular Excitation Energies, Transition Probabilities, and Excited State Properties. *J. Chem. Phys.* **1993**, *98*, 7029−7039.
(30) Radzig, A. A.; Smirnov, B. M. *Reference Data on Atoms, Molecules, and Ions*; Springer Verlag: Berlin, 1985.
(31) Huber, S. E.; Mauracher, A. On the Formation of (Anionic) Excited Helium Dimer in Helium Droplets. *J. Phys. Chem. A* **2014**, DOI: 10.1021/jp503643r.
(32) Hartmann, M.; Miller, R. E.; Toennies, J. P.; Vilesov, A. Rotationally Resolved Spectroscopy of SF_6 in Liquid Helium Clusters: A Molecular Probe of Cluster Temperature. *Phys. Rev. Lett.* **1995**, *75*, 1566−1569.
(33) Brunger, M. J.; Buckman, S. J.; Allen, L. J.; McCarthy, I. E.; Ratnavelu, K. Elastic Electron Scattering from Helium: Absolute Experimental Cross Section, Theory and Derived Interaction Potentials. *J. Phys. B: At. Mol. Opt. Phys.* **1992**, *25*, 1823−1838.
(34) St. Arnaud, J. M.; Bose, T. K. Direct Determination of the Intermolecular Interaction Contribution to the Refractive Index of Carbon Dioxide and Sulfur Hexafluoride. *J. Chem. Phys.* **1979**, *71*, 4951−4955.
(35) Pople, J. A.; Head-Gordon, M.; Raghavachari, K. Quadratic Configuration Interaction—A General Technique for Determining Electron Correlation Energies. *J. Chem. Phys.* **1987**, *87*, 5968−5975.
(36) Maris, H. J. Electrons in Liquid Helium. *J. Phys. Soc. Jpn.* **2008**, *77*, 111008−12.
(37) An der Lan, L.; Bartl, P.; Leidlmair, C.; Schöbel, H.; Jochum, R.; Denifl, S.; Märk, T. D.; Ellis, A. M.; Scheier, P. The Submersion of Sodium Clusters in Helium Nanodroplets: Identification of the Surface → Interior Transition. *J. Chem. Phys.* **2011**, *135*, 044309−6.
(38) Toennies, J. P.; Vilesov, A. F. Superfluid Helium Droplets: A Uniquely Cold Nanomatrix for Molecules and Molecular Complexes. *Angew. Chem., Int. Ed.* **2004**, *43*, 2622−2648.
(39) Woon, D. E.; Dunning, T. H., Jr. Gaussian Basis Sets for Use in Correlated Molecular Calculations. IV. Calculation of Static Electrical Response Properties. *J. Chem. Phys.* **1994**, *100*, 2975−2988.
(40) Boys, S. F.; Bernardi, F. Calculation of Small Molecular Interactions by Differences of Separate Total Energies—Some Procedures with Reduced Errors. *Mol. Phys.* **1970**, *19*, 553−566.
(41) Frisch, M. J.; Trucks, G. W.; Schlegel, H. B.; Scuseria, G. E.; Robb, M. A.; Cheeseman, J. R.; Scalmani, G.; Barone, V.; Mennucci, B.; Petersson, G. A.; et al. *Gaussian 09*, Revision D.01; Gaussian, Inc.: Wallingford, CT, 2009.